THE NCEP WRF CORE

Zavisa Janjic*, Tom Black, Matthew Pyle, Hui-ya Chuang, Eric Rogers and Geoff DiMego
National Centers for Environmental Prediction, Camp Springs, Maryland

1. INTRODUCTION

With constantly increasing horizontal resolution, numerical weather prediction models are approaching limits of validity of the hydrostatic approximation. Although considerable experience with nonhydrostatic models has been accumulated on the scales of convective clouds and storms, numerical weather prediction (NWP) deals with motions on a much wider range of temporal and spatial scales. Having in mind these considerations, a novel approach (Janjic et al., 2001; Janjic, 2003) has been applied in the NCEP Nonhydrostatic Mesoscale Model (NMM) that has been developed within the Weather Research and Forecasting (WRF) initiative. Namely, instead of extending cloud models to larger scales, the hydrostatic approximation is relaxed in a hydrostatic formulation based on modeling principles established by Janjic (1977, 1979, 1984) and proven in NWP practice and regional climate studies. By relaxing the hydrostatic approximation the applicability of the formulation is extended to nonhydrostatic motions, while preserving its favorable features. Thus, the nonhydrostatic NWP model is built on NWP experience.

With this approach the nonhydrostatic equations are split into two parts: (a) the part that corresponds to the hydrostatic system, except for corrections due to the vertical acceleration, and (b) the part that allows computation of the corrections appearing in the first system. No linearization or additional approximation is required. Note that the separation of the nonhydrostatic terms shows in a transparent way how the hydrostatic approximation affects the equations. Moreover, the nonhydrostatic effects are introduced as an add–on module that can be turned on or off. In this way the hydrostatic and nonhydrostatic solutions can be compared, or the model can be run in the hydrostatic mode at lower resolutions with no extra cost.

The considered system of nonhydrostatic equations and the methods for their solving are presented in Janjic et al. (2001), Janjic (2003) and Janjic et al. (2004). Here, only the basic principles of the discretization and some examples of model performance will be reviewed.

2. CLASSICAL NONHYDROSTATIC SOLUTIONS

In order to test the validity of the approach in the limit of highly nonhydrostatic flows, a two-dimensional model in the vertical plane was developed and run in a series of classical nonhydrostatic tests (cf. Janjic et al., 2001). Following Straka et al. (1993), in a neutrally stratified atmosphere an initial cold disturbance was introduced. The horizontal resolution was 100 m, and the vertical resolution was 100 m on the average. The potential temperatures after 300 s, 600 s and 900 s are displayed in Fig. 1. The area shown extends from the center of the domain to 19200 m to the right, and from the surface to 4600 m. The contour interval is $1^0 K$. Comparison of the results with the converged reference solution reveals a very good agreement.

In the warm bubble test a warm initial disturbance was introduced in a neutral atmosphere. The horizontal resolution was 100 m, and the vertical resolution was

100 m on the average. The potential temperature deviations after 360 s, 540 s, 720 s and 900 s are presented in Fig. 2. The area shown extends 16 km
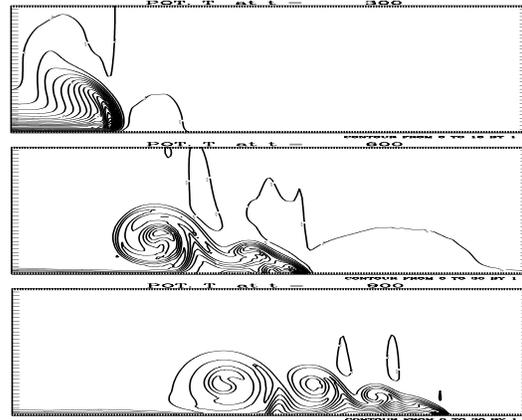

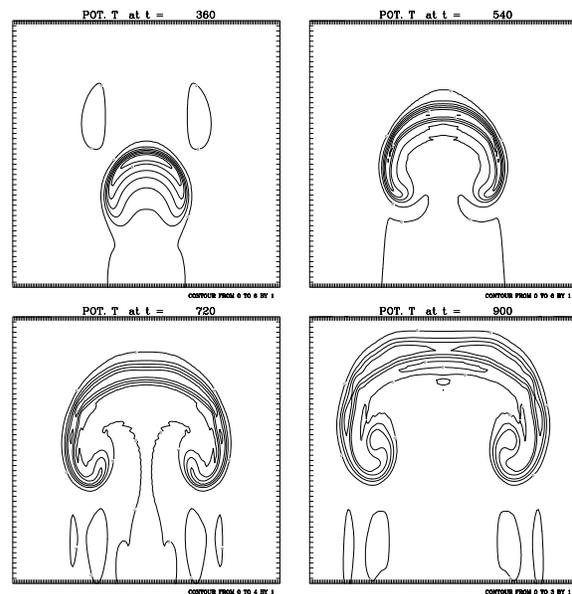Fig. 1. Potential temperature deviation after 300 s, 600 s and 900 s. The contour interval is $1^0 K$.

Fig. 2. Potential temperature deviation after 360 s, 540 s, 720 s and 900 s. The contour interval is $1^0 K$.

along the x axis, and from 1000 m to 13200 m along the z axis. The contour interval is $1^0 K$. The rate of ascent and the intensity of the disturbance agree with those reported elsewhere.

3. DISCRETIZATION

The basic discretization principles applied in the NMM, and thoroughly tested in NWP applications, have been (Janjic, 1977, 1979, 1984, 2003; Janjic et al., 2004):

● Conservation of selected integral properties, and in particular, following Arakawa, the control over the nonlinear energy cascade by the conservation of energy and enstrophy in case of nondivergent flow;
● Cancellation of the contributions of the pressure gradient force and the $\omega\alpha$ term of the thermodynamic equation to the total energy generation, and consequently consistent transformation between the kinetic and potential energy; and
● Minimization of the errors due to sloping vertical coordinate surfaces.

The numerical algorithms following these principles have been developed for the semi-staggered Arakawa grids B and E. For historical reasons, the first version of the NMM was formulated on the E grid. However, a B grid version of the model (NMM-B) also exists (Janjic, 2003). In the vertical, the hybrid pressure-sigma coordinate (Arakawa and Lamb, 1977) is used. It is assumed that the nonhydrostatic pressure deviation vanishes at the top of the atmosphere, while its vertical derivative vanishes at the bottom (Janjic et al., 2001).

The forward–backward scheme (Ames, 1969; Gadd, 1974; Janjic, 1979) is used for the gravity waves and the Adams-Bashforth scheme is used for horizontal advection and for the Coriolis force. For the vertical advection, the Matsuno scheme has been replaced in later versions of the NMM by the unconditionally stable Crank-Nicholson scheme. The implicit scheme is used for vertically propagating sound waves.

In most applications, upgraded physical package of the Eta model has been used. However, the NCAR WRF physical package can be used as well.

4. THE NONLINEAR DYNAMICS OF THE NMM

Nastrom and Gage (1985) examined measurements from commercial aircraft in the lower stratosphere and the upper troposphere. They found that 1D kinetic energy spectra at these altitudes follow the –3 slope on the larger scales, and the –5/3 slope in the range from several hundred kilometers to several kilometers.

The NMM and the NMM-B are well qualified for investigating atmospheric spectra. They conserve energy and enstrophy, which generally improves the accuracy of nonlinear dynamics. In particular, the energy and enstrophy conservation controls the nonlinear energy cascade and restricts spurious energy transfer toward smaller scales by nonlinear interactions. The energy conservation improves the stability of the model and eliminates the need for excessive dissipation that could affect the spectra generated by the model. In addition, the hybrid pressure-sigma vertical coordinate minimizes errors due to sloping vertical coordinate surfaces. Finally, the major dissipative processes are explicit and therefore highly controllable.

The time averaged spectrum over forecast hours 36-48 at 300 hPa (blue diamonds) obtained in the NMM run in the East domain for the case of hurricane Isabel (initial data September 17, 18Z, from the Eta data) with the resolution of 8 km and 60 levels is shown in Fig. 3. The –3 (purple squares) and –5/3 (yellow triangles) slopes are also shown for comparison. The time averaged spectrum over forecast hours 36-48 at 300 hPa (blue diamonds) obtained in a NMM B run over Atlantic is shown in Fig. 4 using the same arrangement. The NMM B was run in a domain of the same size using the resolution of 15 km in the horizontal and 32 levels in the vertical. As can be seen from the figures, the spectra spun up by the model agree remarkably well with the observed Nastrom and Gage (1985) spectrum, even at the rather coarse 15 km resolution.
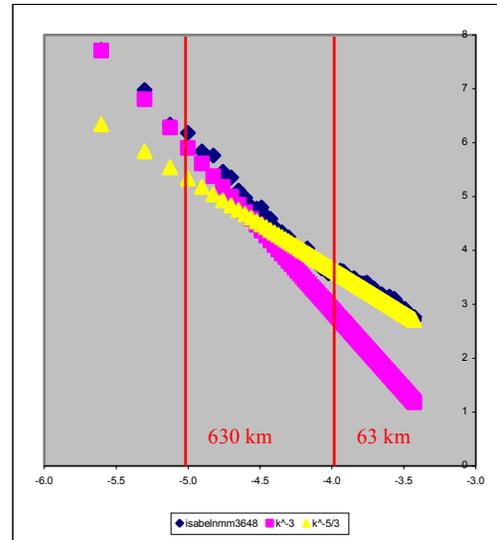

Fig. 3. Time average over 36-48 hours of the NMM spectra (blue diamonds) at 300 hPa in the East domain.
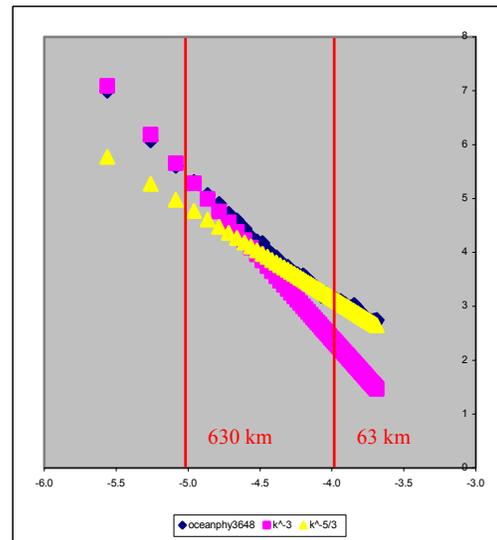

Fig. 4. Time average over 36-48 hours of the NMM B spectra (blue diamonds) at 300 hPa over Atlantic.

In order to examine how the nonlinear dynamics reproduce the spectrum in the case of 3D turbulence, the NMM B was run with horizontal resolution of 1 km, and an average vertical resolution of about 500 m. The horizontal domain had 112 by 112 points. Double periodic boundary conditions were specified along the lateral boundaries. The model was initialized with the vertical thermodynamic structure of the Fort Sill storm of May 20, 1977, and the initial wind field was set to zero. The spectrum of w^2 at the 700 hPa level corresponding to decaying turbulence generated by moist convection was obtained by averaging the spectra between forecast hours 3 and 4. The time averaged spectrum (blue diamonds) is shown in Fig. 5. For comparison, the –5/3 slope (yellow triangles) is also shown. As can be seen from the figure, the agreement between the computed and the theoretical spectrum is again very good.
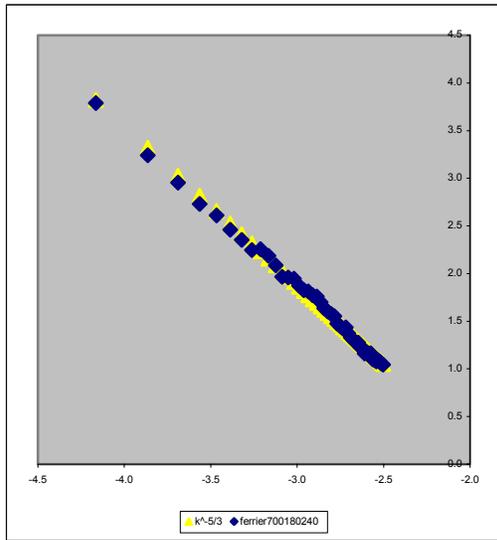
Fig. 5. Decaying 3D turbulence, average over hours 3-4 of the NMM B spectra of w^2 (blue diamonds) at 700 *hPa*.

5. OPERATIONAL APPLICATIONS AND EXPERIMENTAL RUNS

Since July 2002, the NMM has been run operationally in NCEP High Resolution windows. The horizontal resolution is 8 *km* for all domains except for the Alaska domain where the horizontal resolution is 10 *km*. The model has 60 unequally spaced levels in the vertical. The forecasts are computed up to 48 hours. In addition, the model is used for fire weather forecasting and other purposes on call.

The computational efficiency of the model is substantially higher than the computational efficiency of most nonhydrostatic models. Further significant improvement of the computational efficiency is possible. The model has been very reliable in operations.

Generally, the model has been highly competitive with mature operational high-resolution models, despite the fact that it has been handicapped by inconsistent initial and boundary conditions taken from the Eta model, relatively small integration domains, and insufficient tuning of the physical package. Even so, statistical scores and numerous examples (Black et al., 2002, Janjic et al. 2004) indicate that the NMM adds value to the forecasts of the driving Eta model. This applies particularly to the details of flow over complex terrain.

An experimental 12 hour forecast of the sea level pressure starting from September 17, 2003, 12Z is shown in Fig. 6. This forecast covers a part of the life cycle of the tropical storm Isabel. The NCEP GFS data were used to specify the initial and boundary conditions for the NMM. As can be seen from Fig. 6, the predicted pressure in the center of the storm was 951.72 *hPa*, while the observed value was 953 *hPa*. The 30 hour forecast of the accumulated 3 hour precipitation for this case is shown in Fig. 7. The landfall occurred at about this forecast time, and, as can be seen from Fig. 7, it was rather accurately predicted by the model. These examples demonstrate that the NMM has the ability to spin up and maintain realistically deep tropical storms and to accurately predict their tracks.
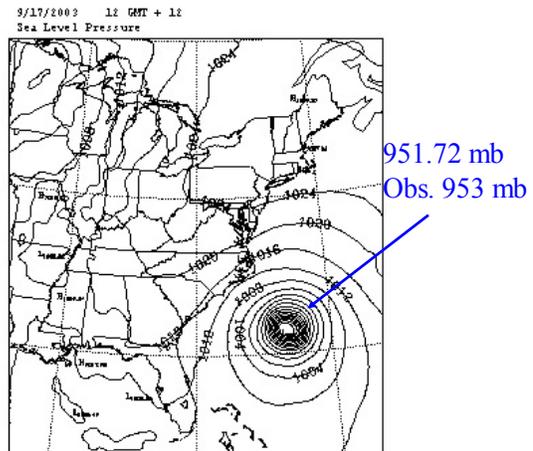

Fig. 6. An experimental 12 hour forecast of the sea level pressure starting from September 17, 2003, 12Z.
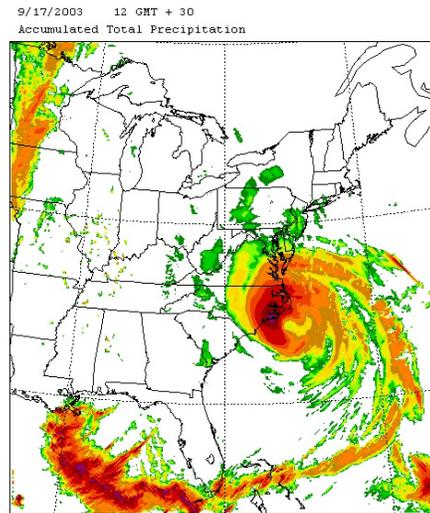

Fig. 7. The 30 hour forecast of the accumulated 3 hour precipitation indicating the location of the landfall.

The example shown in Fig. 8 is from NCEP's experimental 4.5 km resolution runs in support of the Storm Prediction Center (SPC) Spring Program. These forecasts are run once a day up to 30 hours ahead starting from 00Z data with disabled cumulus convection. The 24 hour forecast of accumulated 1 hour precipitation valid at 00Z April 21 is shown in the upper panel of Fig. 9, while the verifying radar reflectivity is shown in the lower panel (Courtesy of Jack Kain). As can be seen from the figure, the predicted precipitation pattern and timing were remarkably similar to the verification.

Finally, the vertical cross section of condensate shown in Fig. 9 is taken from a simulation of the Fort Sill storm (May 20, 1977) using the NMM-B. The horizontal resolution was 1 *km*, and the vertical resolution was about 500 *m* on the average. The integration domain was covered by 112 by 112 grid points.
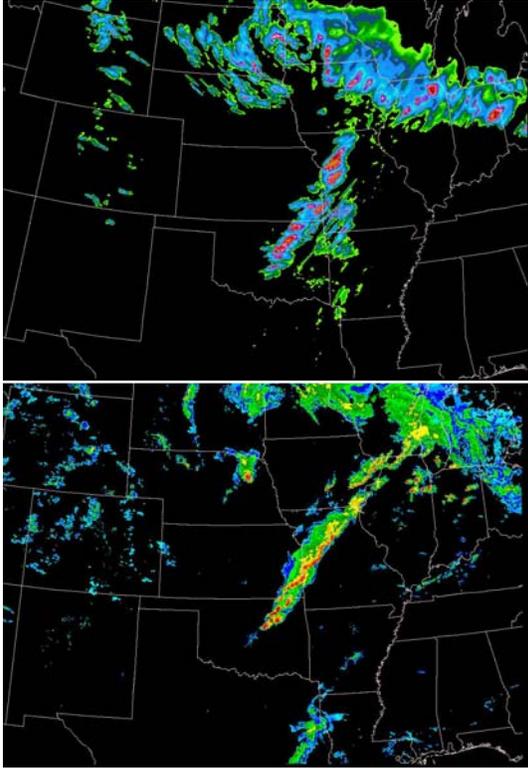
Fig. 8. The 24 hour forecast of accumulated 1 hour precipitation (upper panel) and verifying radar reflectivity (lower panel). (Courtesy of Jack Kain)
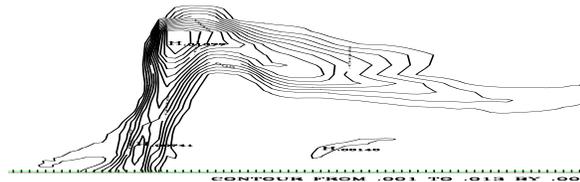

CONTOUR FROM .001 TO .013 BY .00

Fig. 9. Vertical cross section of condensate.

6.   CONCLUSIONS

The NCEP nonhydrostatic mesoscale model (NMM) was formulated building on the experiences of high resolution NWP. The nonhydrostatic dynamics are introduced through an add–on module that can be turned on or off. This allows easy comparison of hydrostatic and nonhydrostatic solutions of otherwise identical model. Also, the model can be run in the hydrostatic mode at lower resolutions with no extra cost.

At very high resolutions, a two-dimensional version of the model successfully reproduced classical nonhydrostatic solutions. Although such resolutions will not be affordable in NWP applications in the near future, it was necessary to pass these tests in order to demonstrate the soundness of the formulation.

The nonlinear dynamics of the NMM demonstrated the ability to reproduce the observed atmospheric spectrum. Moreover, at higher resolution, the NMM reproduced the theoretical 3D spectrum in the case of decaying three-dimensional turbulence.

The extra computational cost due to the nonhydrostatic dynamics is of the order of 20% of the cost of the hydrostatic dynamics. The relatively low cost of the nonhydrostatic dynamics justifies its application even at medium resolutions. Compared to the hydrostatic version of the model, no additional computational boundary conditions at the top have been needed in real data runs in a wide range of horizontal resolutions.

The NMM has become operational at NCEP in July of 2002 and has demonstrated a high level of skill and ability to add value to the forecasts produced by the driving model. Despite the application of sophisticated numerical methods, the computational efficiency of the model is very high, and substantially higher than the computational efficiency of most nonhydrostatic models. The model has been very reliable in the operations.

Further efforts are needed in order to develop full potentials of the model. This applies primarily to modifications and retuning of the physical parameterizations.

REFERENCES

Ames, W.F., 1969: Numerical Methods for Partial Differential Equations. *Nelson*, London, 291 pp.

Arakawa, A. and V. R. Lamb, 1977: Computational design of the basic dynamical processes of the UCLA general circulation model. Methods in Computational Physics, 17, Academic Press, 173-265.

Black, T., E. Rogers, Z. Janjic, H. Chuang, and G. DiMego, 2002: Forecast guidance from NCEP's high resolution nonhydrostatic mesoscale model. 15th Conf. on NWP, San Antonio, TX, Amer. Meteor. Soc., J23-J24.

Gadd, A.J., 1974: An economical explicit integration scheme. Meteorological Office Techn. Note 44, 7 pp. London Road, Bracknell, Berks. RG12 2SZ, U.K.

Janjic, Z. I., 1977: Pressure gradient force and advection scheme used for forecasting with steep and small scale topography. *Contrib. Atmos. Phys.*, **50**, 186–199.

_____, 1979: Forward–backward scheme modified to prevent two–grid–interval noise and its application in sigma coordinate models. *Contrib. Atmos. Phys.*, **52**, 69–84.

_____, 1984: Non–linear advection schemes and energy cascade on semi–staggered grids. *Mon. Wea. Rev.*, **112**, 1234–1245.

_____, 2003: A Nonhydrostatic Model Based on a New Approach. *Meteorol. Atmos. Phys.*, **82**, 271-285.

Janjic, Z. I., J. P. Gerrity, Jr. and S. Nickovic, 2001: An Alternative Approach to Nonhydrostatic Modeling. *Mon. Wea. Rev.*, **129**, 1164-1178.

Janjic, Z., T. Black, M. Pyle, H. Chuang, E. Rogers and G. DiMego, 2004: An Evolutionary Approach to Nonhydrostatic Modeling. Symposium on the 50th Aniversary of Operational Numerical Weather Prediction, College Park, MD, Amer. Meteor. Soc.

Nastrom, G.D., Gage, K.S., 1985: A Climatology of Atmospheric Wavenumber Spectra of Wind and Temperature Observed by Commercial Aircraft. *J. Atmos. Sci*, **42**, 950–960.

Straka, J.M., R.B. Wilhelmson, L.J. Wicker, J.R. Anderson and K.K. Droegemeier, 1993: Numerical solutions of a non-linear density current: a benchmark solution and comparisons. *Intl. J. Numerical Methods in Fluids*, **17**, 1-22.